# A Novel Capacitive Safety Device for Target Localization and Identification

Bernard Pottier, Lanto Rasolofondraibe, and Danielle Nuzillard, *Member, IEEE*

***Abstract*—A novel capacitive device dedicated to the safety of people working on automated production sites has been developed. It can be implemented on an articulated mechanical system (robot, press) to estimate the distance between sensors that are fixed on such a system and a mobile target. An interdigital sensor has been fabricated to identify the target nature among them (human beings or objects). The variable geometry of the system is taken into account as well as its motion relatively towards the ground by means of an ingenious sensitive element design. Furthermore, the sensors are made of conducting paint, thus providing low weight and negigible space hindrance devices. Results show this novel low cost sensing set-up has a great potential to estimate the distance and to discriminate targets. This work is patented to the INPI (National Institute of Intellectual Protection) under the number: n°2898825, 2007.**

***Index Terms*—Capacitive sensor, safety device, target discrimination.**

## I. Introduction

In recent years, robots were implemented increasingly on production sites. To prevent new risks of accidents, new security equipments and methodologies [1], have been developed. However, safety is not completely ensured during the interventions when some protections must be neutralized. With this aim in view, a new safety device [2] has been developed, it is based on the properties of the electric field and capacitance variations [3]. Its main purpose is to detect and to locate an operator or an object in a non protected area. Initially such principle of detection was implemented on dangerous machines for which the geometry is well-defined and the operating mode is *all or nothing* compared to an appropriated safety threshold [4]. In robotics the geometry is variable then the capacitance variations of the system on itself must be considered.

To identify a target : human being or object, and to locate it around a robot, its geometry and the physical phenomena related to the target-sensor couplings are essential [1], [5]–[8], as well as the implementation of the sensors [3], [9], [10].

Section 2 deals with the underlying theory of capacitive couplings and the measurement of its coefficients. In section 3, theoretical and functional models have been designed and validated experimentally. In section 4, the device has been implemented to detect an intruder and experimental results are reported. In section 5, the indetermination related to the distance and to various intruders type discrimination has been solved, experimental results are reported, too. Section 6 deals with practical considerations to make an efficient sensor.

The authors are with the Centre de Recherche en Sciences et Technologie de l'Information et de la Communication, University of Reims Champagne-Ardenne, CReSTIC URCA, Moulin de la Housse, BP 1039, 51089 Reims Cedex2, France (e-mail: bernard.pottier@univ-reims.fr, lanto.rasolofondraibe@univ-reims.fr, danielle.nuzillard@univ-reims.fr).

Manuscript received July 6, 2007; revised December 18, 2007; accepted January 21, 2008. The associate editor coordinating the review of this paper and approving it for publication was Dr. Subhas C. Mukhopadhyay.

January $30^{th}$, 2007

## II. Capacitive Coupling

### A. Principe

A single conductor connected to a voltage source $V(t)$ receives a quantity of electric charges $Q(t)$. According to Coulomb's law, electric charges with the same sign repel each other and the balance is obtained for the ratio in Eq.1:

$$C_{S\infty} = \frac{Q(t)}{V(t)} \tag{1}$$

where $C_{S\infty}$ is the coefficient of capacitance of that single conductor in the space. The set {conductor, infinity} can be viewed as a capacitor. Electric charges $Q(t)$ generate an electric field whose lines are normal to the conductor surface and diverge far away.

Consider a system of $n$ conductors. At each time, its equilibrium is characterized by the set of electric charges $\{Q_1(t), ..., Q_n(t)\}$ and the set of voltages $\{V_1(t), ..., V_n(t)\}$ as shown in Fig.1(a). In stationary state, the charges are related to the voltages by linear equations Eq.2.

$$Q_i(t) = \sum_{j=1}^{n} C_{ij}.V_j(t) \quad \text{or} \quad Q = CV \tag{2}$$

$C_{ij}$ is the coefficient of capacitance of the $j^{th}$ conductor on the $i^{th}$, it depends only on the geometry of the system, then $C_{ij} = C_{ji}$. $C_{ii}$ is the own capacitance of the $i^{th}$ conductor surrounded by the others. In a matrix form, $C$ is symmetric. Coefficients fulfill the condition in Eq.3.

$$C_{ii} \geq |\sum_{i \neq j} C_{ij}| \tag{3}$$

If all the conductors are grounded, they are inactive and they do not emit any field. If only one conductor is active (fixed at $V_1 \neq 0$), its charges emit an electric field as shown in Fig.1(b), the others are inactive ($V_i = 0, i \neq 1$), but only reactive to the emitted field. The ground is a good origin for the potential. The equilibrium state is reached when :

$$\begin{bmatrix} Q_1(t) \\ Q_2(t) \\ ... \\ Q_n(t) \end{bmatrix} = \begin{bmatrix} C_{11} & C_{12} & ... & C_{1n} \\ C_{21} & C_{22} & ... & C_{2n} \\ ... & ... & ... & ... \\ C_{n1} & C_{n2} & ... & C_{nn} \end{bmatrix} \begin{bmatrix} V_1(t) \\ 0 \\ ... \\ 0 \end{bmatrix} \tag{4}$$

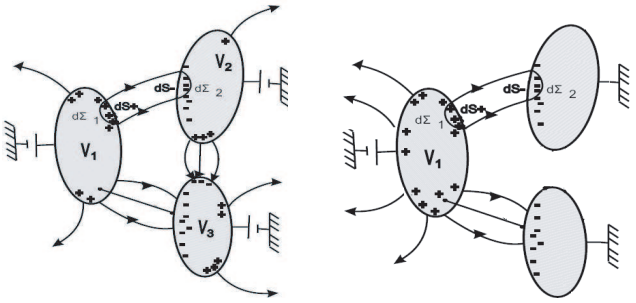


(a) Each conductor 'i' at $V_i \neq 0$ (b) $V_1 \neq 0$, $V_2 = 0$, $V_3 = 0$

Fig. 1. Mutual influence of conductors.

then

$$Q_1(t) = C_{11}.V_1(t) \quad \text{and} \quad Q_i(t) = C_{i1}.V_1(t) \tag{5}$$

$$C_{11} = \frac{Q_1(t)}{V_1(t)} \quad \text{with} \quad Q_1(t) = \int_{S_1} \sigma_1(t) dS_1 \tag{6}$$

where $\sigma_1(t)$ is the superficial charge density of the $1^{st}$ conductor.

### B. Capacitive Coupling Analysis

Consider a single conductor playing the role of a sensor, its voltage source is $V_1(t) = V_0 sin(2\pi ft)$. Far from any other conductor its charge is $Q_1(t)$ such as :

$$C_{11} = \frac{Q_1(t)}{V_1(t)} = C_{1s}(d \to \infty) \tag{7}$$

where $C_{1s}(d \to \infty)$ (denoted $C_{1s\infty}$ for the sake of simplicity) is its own capacitance that is depending only on its geometry and its surface. Assume a second conductor playing the role of a grounded target. The closer the target is, the more the electric field interacts with it, and it appears a coupling $C_{12}(d)$ between them. However if the sensor and the target would have constitute an isolated system, the new sensor charges, denoted by $Q_1^{'}(t)$, would decrease compared to the initial charge $Q_1(t)$. But the sensor is fixed at $V_1(t)$, then new charges $q(t)$ are injected to maintain the equilibrium such as $C_{1s}(d)$ and $C_{11}$ are :

$$C_{1s}(d) = \frac{Q_1'(t)}{V_1(t)} \quad \text{with} \quad Q_1'(t) < Q_1(t) \tag{8}$$

$$C_{11} = \frac{Q_1'(t) + q(t)}{V_1(t)}. \tag{9}$$

Consequently, while the target is approaching [11], $C_{1s}(d)$ is decreasing, $C_{12}(d)$ is increasing and $C_{11}(d)$ is increasing as drawn in Fig.2.

$$C_{11}(d) = C_{1s}(d) + C_{12}(d) \tag{10}$$

$$0 \leq C_{1s}(d) \leq C_{1s\infty} \tag{11}$$

$$C_{12\infty} = 0 \leq C_{12}(d) \tag{12}$$

Now assume an intruder coming near this set composed of a sensor [7], [8] and a target, $C_{11}(d,t)$ can be written as follows:

$$C_{11}(d) = C_{1s}(d) + C_{12}(d) + C_{int}(d) \tag{13}$$

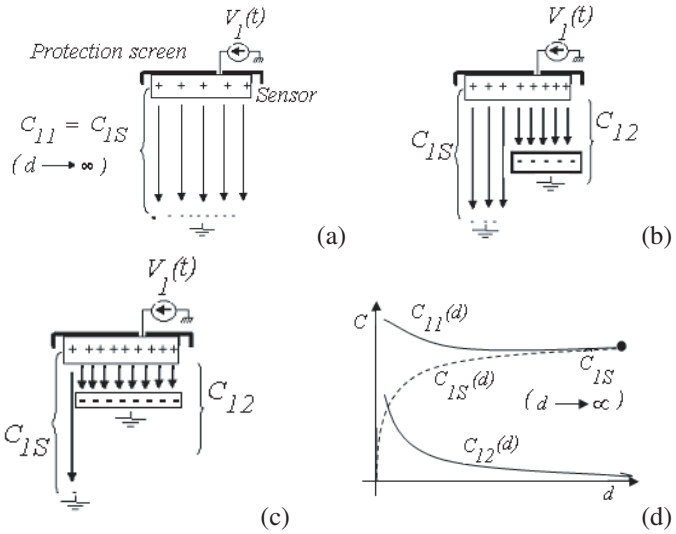


Fig. 2. Capacitance behavior of $C_{11}$; a, b, c: Qualitative components of $C_{11}$, sensor - grounded target; d: $C_{1s}$, $C_{11}$ and $C_{12}$ versus distance curves.

where $C_{int}(d)$ is the capacitance between the sensor and the intruder. Then the intruder detection requires to know the evolution of $C_{11}(d)$, $C_{1s}(d)$, $C_{12}(d)$. The system is generalizable to $n$ conductive sensors as written in Eq.14 and in Fig.3.

$$C_{ii}(d) = C_{is}(d) + \sum_{j=1, i\neq j}^{n} C_{ij}(d) + C_{int}(d) \tag{14}$$

$$C_{int}(d) = C_{ii}(d) - C_{is}(d) - \sum_{j=1, i\neq j}^{n} C_{ij}(d) \tag{15}$$

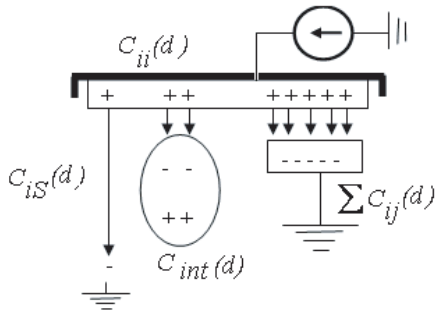


Fig. 3. Intruder close to the system.

### C. Measurement of the Coupling Coefficient $C_{11}$

To measure $C_{11}$, the sensor must be inserted in an electronic circuit as shown in Fig.4. Since the goal is to translate the evolution of the sensor capacitance [12], input impedances of the linear integrated amplifier must be very high. The amplifier OPA 129 [13] is used because its bias currents are less than 30 fA and its input capacitances less than 1 pF. These characteristics are compulsory because the current variations $\Delta i(t)$ and the capacitances are comprised between:

$$0.1\text{pA} \leq \Delta i(t) \leq 100\text{pA}$$

$$0.1\text{pA} \leq \Delta C_{11}(d) \leq 20\text{pA}$$

A non-inverting linear differentiator is implemented, it behaves like a "pump of charges". The sensor constitutes the first plate

of a capacitor while the second plate is rejected far away at the ground potential. The relationship between $C_{11}$ and the output $V_{out1}$ is given in Eq.16 where $t$ is omitted for the sake of simplicity.

$$\begin{aligned} V_{out1} &= V_i n\sqrt{1+(R\omega C_{11})^2} \\ &= V_e\sqrt{1+(R\omega(C_{1s}(d)+C_{21}))^2} \end{aligned} \quad (16)$$

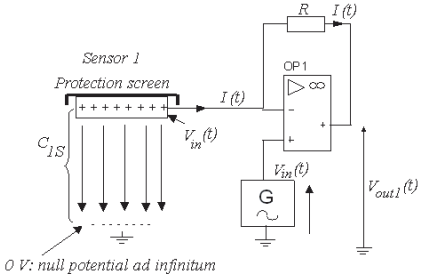


Fig. 4. Capacitive coupling and access to $C_{11}$.

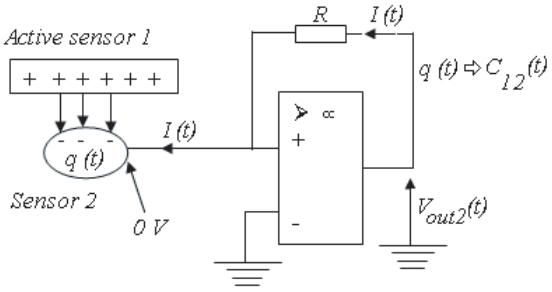


Fig. 5. Capacitive coupling and access to $C_{12}$.

### D. Measurement of the Inductance Coefficient: $C_{12} = C_{21}$

The intruder can be a human being, an object or a part of the mobile system itself that is also equipped with a sensor called sensor 2 or target; this one being in regard with the sensor 1. To measure the value of $C_{12} = C_{21}$, the sensor 2 is virtually grounded and it is inserted in an electronic circuit as shown in Fig.5. Again, far from any active sensor, it is not charged and its own capacitor $C_{2S\infty}$ (single target only) is not translated then the output voltage is $V_{out2}(t) = 0$ V. When the sensor 2 is induced by the sensor 1, according to the theorem of the corresponding elements, all the charges in equal quantity but of opposite sign repel charges from the sensor 1. Consequently, the measurement of $V_{out2}(t)$ gives access to $C_{12}$ since:

$$V_{out2} = V_{in}R\omega C_{12} \quad (17)$$

It is noticeable that the sensor 2 remains inactive with respect to others neutral targets since it is grounded virtually and it does not emit any electric field.

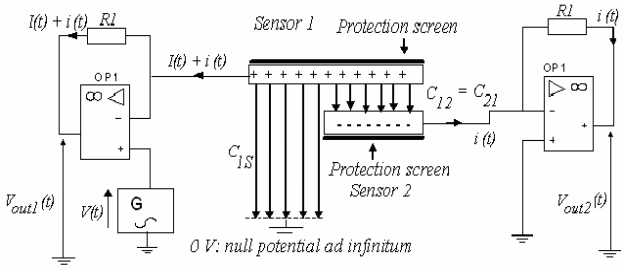


Fig. 6. Implementation scheme of the capacitive coupling translation.

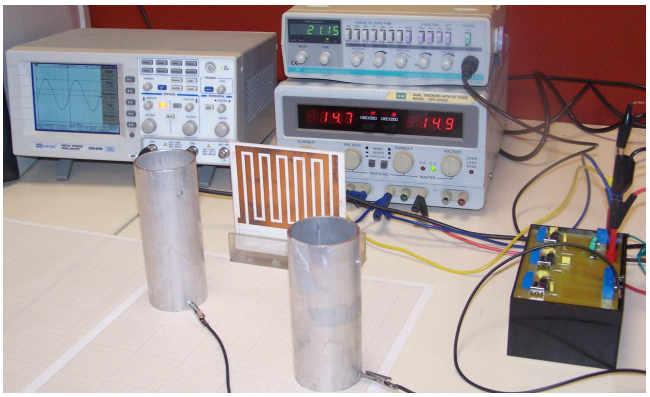

Fig. 7. Fabricated interdigital set-up and its associated electronic.

## III. Modelling and Experimental Validation

### A. One active sensor solely

Fig.6 shows the schematic implementation of previous circuits and the experimental set-up is displayed in Fig.7.
Two electric potentials $V_{out1}$ and $V_{out2}$ are available, they translate the evolution of the capacitance of each sensor according to the distance $d$ between them as previously written (*vide supra*). The value of $C_{1S\infty}$ decreases when the field lines meet a target. Combination of Eq.16 and Eq.17 gives $C_{11}$ and $C_{12}$ as follows:

$$C_{11} = C_{1s}(d) + C_{21} = \frac{1}{V_{in}R\omega}\sqrt{V_{out1}^2 - V_{in}^2} \quad (18)$$

$$C_{12} = C_{21} = \frac{1}{V_{in}R\omega}V_{out2}. \quad (19)$$

Their difference leads to an experimental model which links $C_{1s}(d)$, $V_{out1}$ and $V_{out2}$ as written in Eq.20.

Experimental Model:

$$\begin{aligned} C_{1s}(d)_{exp} &= C_{11} - C_{21} \\ &= \frac{1}{V_{in}R\omega}(\sqrt{V_{out1}^2 - V_{in}^2} - V_{out2}) \end{aligned} \quad (20)$$

At the same time, an intuitive reference model was built from the qualitative reflection of the couplings, as written in Eq.21. It fits the experimental model through the adjustment of an empirically determined parameter $\beta$.

Reference Model:

$$\begin{aligned} C_{1s}(d)_{mod} &= C_{1s\infty}(1 - \frac{C_{21}^{\alpha}}{C_{1s\infty} + C_{21}}) \\ \text{with } \alpha &= \frac{C_{1s\infty} + \beta C_{21}}{C_{1s\infty}} \end{aligned} \quad (21)$$

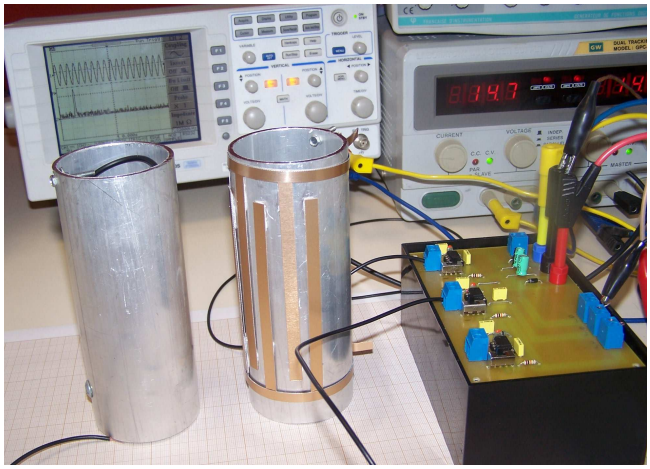

Fig. 8. Fabricated interdigital set-up and associated electronic.

### B. Experimental validation for one active sensor

Both models, the experimental one in Eq.20 and the reference one in Eq.21, were validated according to the following procedure. Two aluminium tubes of 60 mm diameter and 130 mm length simulate two arms of a robot as shown in Fig.8. One was set at the input voltage $V_{in}$ and the other was grounded. The output voltages $V_{out1}$ and $V_{out2}$ were recorded according to the distance $d$ between both sensors. The measures displayed in Fig.9 show that the experimental and theoretical curves are nearly superimposed.

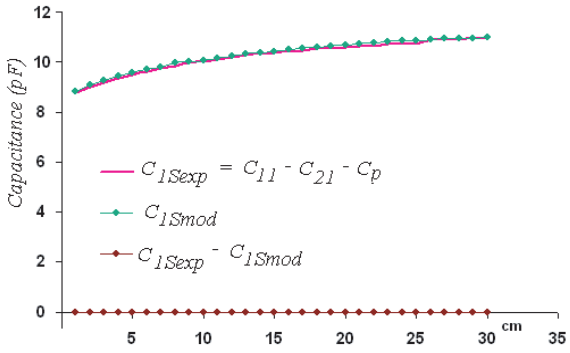


Fig. 9. Experimental model validation, $\beta = 1$, $C_{1Sexp}$ is the experimental capacitance curve, $C_{1Smod}$ is the model, their difference is null, $C_p$ is the capacitor of the shielded connection wire.

### C. Generalization for n sensors

Assume that a robot has $n$ mobile arms and each of them is equipped with a sensor as shown in Fig.10. Eq.20 and Eq.21 become Eq.22 and Eq.23 respectively.

Experimental Model:

$$C_{1s}(d)_{exp} = C_{1i} - \sum_{j=2}^{n} C_{j1} = \frac{1}{V_{in} R\omega}\left(\sqrt{V_{out1}^2 - V_{in}^2} - \sum_{j=2}^{n} V_{outj}\right) \quad (22)$$

Reference Model:

$$C_{1s}(d)_{model} = C_{1s\infty}\left(1 - \frac{\sum_{j=2}^{n} C_{j1}^{\alpha}}{C_{1s\infty} + \sum_{j=2}^{n} C_{j1}}\right) \quad (23)$$

$$\text{with } \alpha = \frac{C_{1s\infty} + \beta \sum_{j=1,2}^{n} C_{j1}}{C_{1s\infty}}$$

As long as no intrusion occurs in the volume scanned by the active sensor, the equality between both models in Eq.22 and Eq.23 is verified.

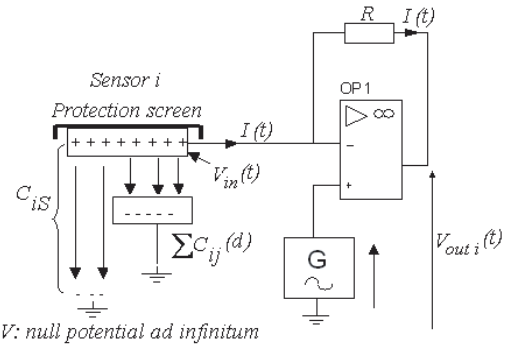


Fig. 10. Coupling translation for $n-1$ passive sensors.

### D. Experimental validation for 3 passive sensors

Both models in Eq.22 and Eq.23 were experimentally validated. Only one sensor was active while the n-1 others were grounded. A mobile sensor was coming close to the active sensor. All output voltages $V_{outj}$ were registered. This procedure was repeated several times by swapping the mobile sensor and its location. Again the experimental and theoretical curves were superimposed confirming the models validity as shown in Fig.11.

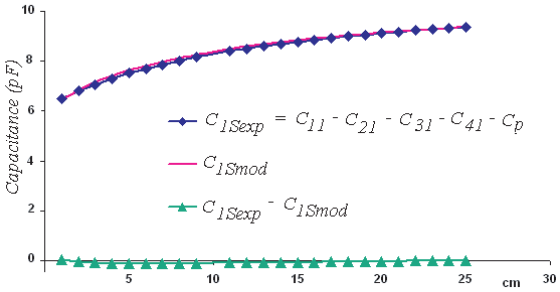


Fig. 11. Experimental model validation, $\beta = 0.2$, $C_{1Sexp}$ is the experimental capacitance curve, $C_{1Smod}$ is the model, their difference is null.

## IV. Detection of an intrusion

### A. Principe

The equality between Eq.22 and Eq.23 is always verified when the active sensor is not disturbed by any intruder since each coefficient $C_{ji}$ depends only on the coupling between the active sensor $i$ and each inactive sensor $j$. When an intrusion occurs, a new coupling is created between the active sensor and the intruder, each $C_{ji}$ is decreased and $C_{1s}(d)_{exp}$ is increased

in Eq.22 while it is unchanged in Eq.23 due to $\alpha$ and the adjusted parameter $\beta$. Thus, this difference makes it possible to detect an intrusion. This difference is larger as far as the intrusion is significant and close to the active sensor.
Now assume the floor is not electrically grounded, and the interaction between the active sensor and the floor is significant. This capacitive effect is considered by spreading out a conducting paint on the floor which plays the role of a grounded sensor. When an intrusion occurs, either it is in contact with the floor or not. Both cases are considered in the following.

### *B. No contact with the floor*

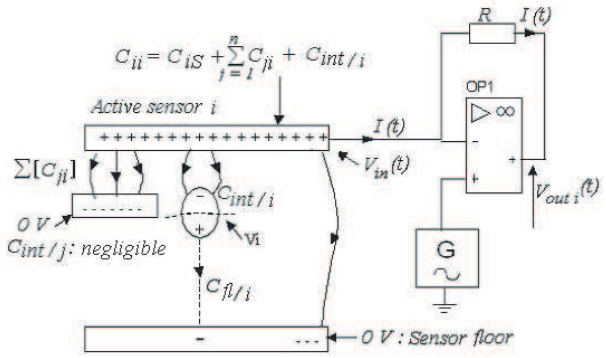


Fig. 12. Intrusion detection.

As in Fig.12, the intruder is not in contact with the floor (far enough), then this latter behaves like any sensor $j$ since it is grounded. The influence of that intrusion on a sensor $j$ is negligible while the supply of the intrusion $V_{int}$ is less than $V_i$ that of the current active sensor $i$, $V_{int} < V_i$. The coupling between the intruder and the active sensor is included in the experimental model in Eq.25.

Experimental Model:

$$V_{outi} = V_e \sqrt{1 + (R\omega)^2 \left( C_{is} + \sum_{i=1, i\neq j}^{n} C_{ji} + C_{int/i} \right)^2} \quad (24)$$

$$\sum_{j=1, j\neq i}^{n} V_{outj} = V_e R\omega \left( \sum_{j=1, j\neq i}^{n} C_{ij} + C_{int/j} \right) \approx V_{in} R\omega \sum_{j=1, j\neq i}^{n} C_{ij}$$

The equality between both models only stands as long as there is no intruder inside the volume under supervision. When an intrusion occurs, curves in Fig.9 and in Fig.11 are no more superimposed, the coupling coefficient $C_{int/i}$ due to the intruder is calculable.

$$C_{int/i} = C_{is}(d)_{exp} - C_{is}(d)_{mod} \quad (25)$$

Fig.13(a) shows the behavior of the coupling coefficients when a man is at 10 cm of an active sensor and Fig.13(b) when the intruder is made in metal.

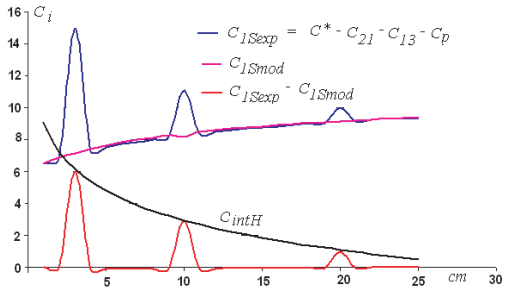


(a) The intruder is a man.

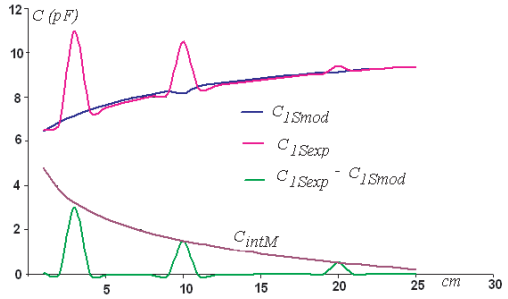


(b) The intruder is a metallic target.

Fig. 13. Experimental results for an intrusion, envelop of $C_{int}$, $C_{1S}$ is the experimental curve, $C_{1Smod}$ is the model, their difference is $C_{1S}$-$C_{1Smod}$.

### *C. Contact with the floor*

When the intrusion is in contact with the floor, the capacitive coupling intrusion-floor is not negligible. To know its value $C_{int/fl}$, it is necessary to ground the active sensor 1 and to activate the sensor floor with a potential $V = 0.1V_{in}$ in order to return all the couplings $C_{ji} = 0$, particularly the couplings $C_{fl/i}$ and $C_{int/i}$ as shown in Fig.14(a) and Fig.14(b). Then $V_{outi}$, $V_{outj}$ and $C_{int/i}$ are given by Eq.26, Eq.27 and Eq.28 respectively.

$$V_{outi} = V_{in} \sqrt{1 + (R\omega)^2 \left( C_{is} + \sum_{i=1, i\neq j}^{n} C_{ji} + C_{int/i} - C_{int/fl} \right)^2} \quad (26)$$

$$V_{outj} = V_e R\omega C_{1j} \quad (27)$$

$$C_{int/i} = C_{is}(d)_{exp} - C_{is}(d)_{mod} - C_{int/fl} \quad (28)$$

## V. Distance Measurements and Targets Discrimination

### *A. Principe*

The coefficient of induction is modeled by $C_{int} = \varepsilon \frac{S}{d_i}$, where $S$ is the surface of an intruder in regard to the active sensor, $d_i$ the distance between these surfaces and $\varepsilon$ the permittivity of the medium between both surfaces. The solely knowledge of $C_{int/i}$ is not sufficient to locate the intrusion since the quantity $\varepsilon.S$ may be large and far away from the active sensor or small and close to it.
To raise this uncertainty, the variation rate $\theta_{int/i} = \frac{\Delta C_{int/i}}{\Delta d}$ has to be estimated. For that two identical sensors [14] are placed one behind the other separated by a distance $\Delta d$ as

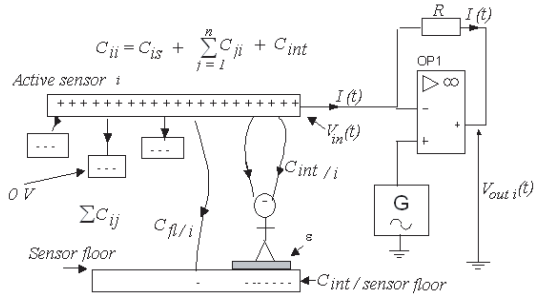


(a) Principe

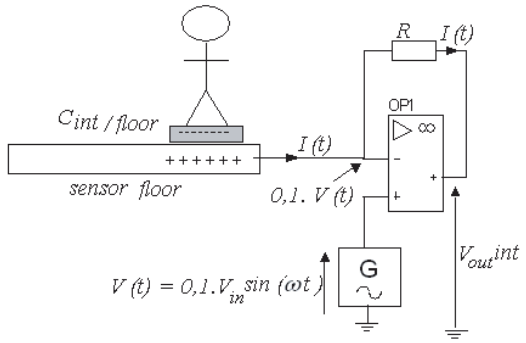


(b) Coupling intrusion/floor

Fig. 14. Detection of an intrusion on the floor.

shown in Fig.15, then $C_{int/i}(d_i)$, $C_{int/i}(d_i+\Delta d)$ and $\Delta d$ are measured.

$$\theta_{int/i} = \frac{\Delta C_{int/i}}{\Delta d} = \frac{C_{int/i}(d_i+\Delta d) - C_{int/i}(d_i)}{\Delta d}$$
$$\theta_{int/i} = \frac{\varepsilon S}{\Delta d}\left(\frac{1}{d_i+\Delta d} - \frac{1}{d_i}\right) \approx -\frac{\varepsilon S}{d_i^2} \qquad (29)$$

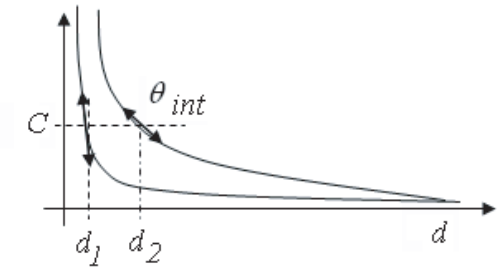


Fig. 15. Localization and discrimination of an intruder.

From $C_{int/i}$ and $\theta_{int/i}$ the intrusion can be locate $(d_i)$ and discriminate $(\varepsilon.S)$ by comparing the measurements made with the active sensor:

$$\left|\frac{C_{int/i}}{\theta_{int/i}}\right| \Rightarrow \varepsilon S \qquad (30)$$

### *B. Experimental Results.*

Different intruders type were tested: a man and a metallic target. Output voltages were registered, $C_{int/i}(d)$, $C_{int/i}(d+\Delta d)$ were calculated according to Eq.28 and are displayed in Fig.16. Then Eq.29 and Eq.30 are used to estimate $\theta$, $d$ and $(eS)$ respectively as seen in Tab.I and Tab.II. The curves $\Delta C$ and $\theta$ versus $d$ are displayed in Fig.17(a) and Fig.17(b).

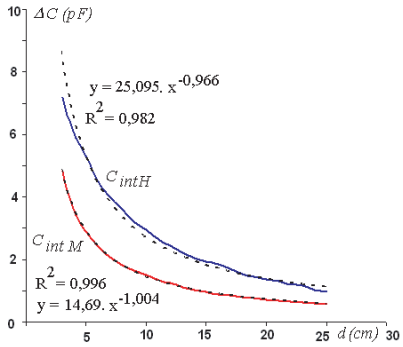


Fig. 16. Experimental results, coupling sensor-intruder versus distance : $Cint_H$ for a human, $Cint_M$ for a metallic target.

TABLE I
HUMAN INTRUSION ($\Delta d = 5$ MM);
LEFT: MEASURES, RIGHT: $d_H$ AND $(\varepsilon.\mathrm{S})_H$ ESTIMATION.

| $d$ | $C_{intH}$ | $C_{intH}.(d+\Delta d)$ |
|---|---|---|
| 3 | 7.2 | 6.171 |
| 4 | 6.1 | 5.422 |
| 6 | 4.5 | 4.154 |
| 8 | 3.6 | 3.388 |
| 10 | 2.943 | 2.803 |
| 12 | 2.456 | 2.358 |
| 14 | 2.0442 | 1.974 |
| 16 | 1.84 | 1.784 |
| 18 | 1.5406 | 1.499 |
| 20 | 1.3609 | 1.328 |
| 22 | 1.2031 | 1.176 |
| 24 | 1.01 | 0.989 |
| 25 | 0.956 | 0.937 |

| $\theta_H$ | $d_H$ | $(\varepsilon.S)_H$ |
|---|---|---|
| 2.06 | 3.50 | 25.20 |
| 1.36 | 4.50 | 27.45 |
| 0.69 | 6.50 | 29.25 |
| 0.42 | 8.50 | 30.60 |
| 0.28 | 10.50 | 30.90 |
| 0.20 | 12.50 | 30.70 |
| 0.14 | 14.50 | 29.64 |
| 0.11 | 16.50 | 30.36 |
| 0.08 | 18.50 | 28.50 |
| 0.07 | 20.50 | 27.90 |
| 0.05 | 22.50 | 27.07 |
| 0.04 | 24.50 | 24.75 |
| 0.04 | 25.50 | 24.38 |

When the intruder is mobile, $(\varepsilon.S)$ fluctuates around the value measured when it was immobile. For a human being, one measures $0.85(\varepsilon.S)_H < (\varepsilon.S)_H < 1.15(\varepsilon.S)_H$.
From the generalized Eq.25 and Eq.25, by successively swapping the role of the active sensor, capacitance couplings between the intruder and the active sensors are measurable. From these measurements, the methods of triangulation as well

TABLE II
METALLIC INTRUSION ($\Delta d = 5$ MM);
LEFT: MEASURES, RIGHT: $d_M$ AND $(\varepsilon.S)_M$ ESTIMATION.

| $d$ | $C_{intM}(d)$ | $C_{intM}(d+\Delta d)$ |
|---|---|---|
| 3 | 4.8426 | 4.151 |
| 4 | 3.6322 | 3.229 |
| 6 | 2.4221 | 2.235 |
| 8 | 1.8185 | 1.712 |
| 10 | 1.4994 | 1.428 |
| 12 | 1.2387 | 1.189 |
| 14 | 1.0182 | 0.985 |
| 16 | 0.8945 | 0.870 |
| 18 | 0.8001 | 0.780 |
| 20 | 0.7222 | 0.705 |
| 22 | 0.6603 | 0.646 |
| 24 | 0.6089 | 0.593 |
| 25 | 0.579 | 0.563 |

| $\theta_M$ | $d_M$ | $\varepsilon.S_M$ |
|---|---|---|
| 1.38 | 3.50 | 16.95 |
| 0.81 | 4.50 | 16.36 |
| 0.37 | 6.47 | 15.68 |
| 0.21 | 8.54 | 15.53 |
| 0.14 | 10.50 | 15.74 |
| 0.10 | 12.46 | 15.44 |
| 0.07 | 15.33 | 15.61 |
| 0.05 | 18.26 | 16.33 |
| 0.04 | 19.90 | 15.92 |
| 0.03 | 20.99 | 15.16 |
| 0.03 | 23.09 | 15.24 |
| 0.03 | 23.09 | 14.61 |
| 0.03 | 19.15 | 11.66 |
| 0.03 | 18.09 | 10.48 |

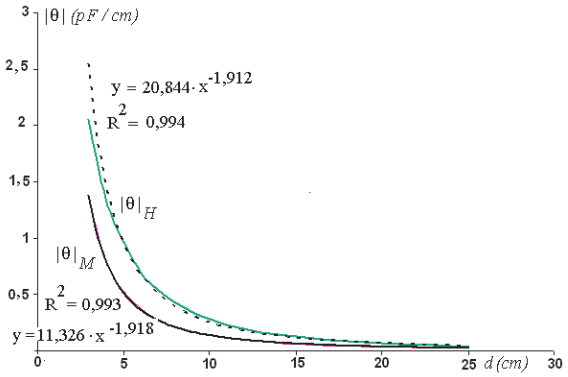


(a) Evaluation of $\theta$ versus distance.

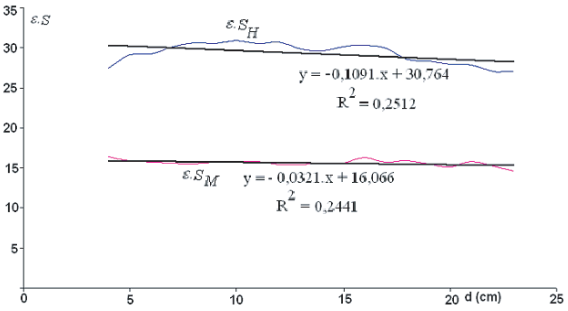


(b) Evaluation of $\varepsilon S$ versus distance.

Fig. 17. Detection of an intrusion on the floor, index $_H$ for a man and $_M$ for a metallic target.

as the knowledge of the articular variables of the robot make it possible to locate and discriminate the intruder.

## VI. Practical considerations

### A. Protection of sensors against internal parasites

The sensors are made with superimposed coats of conducting paint spread out on dangerous parts of the robot because their weight and their space hindrance are negligible. But essential electric components are inside the robot arms such as electric motors, position coders, electronic power or any other electric system. They can generate electromagnetic parasites and disturb the sensors. Moreover moving internal elements can generate inductive couplings with them due to their relative displacement.

To circumvent these effects, it is necessary to form a Faraday's cage at the place where the sensors are implemented. Thus, a first layer of conducting paint was spread out locally, it is fixed at a ground potential when the sensor is inactive and at a potential $V_{in}$ when it is active. A second coat of isolating paint was spread out to insulate the sensor from the Faraday's cage, finally a third coat of conducting paint constitutes a sensitive element of our safety device.

The sensor was insulated from disturbances due to the various internal elements of the robot and the main part of the field that it emits, is directed towards the zones to supervise. Its geometry is adapted according to the objectives to realize. One will be able also if necessary to make a guard ring around it.

### B. Discrimination man/object and distance target

To discriminate targets, both sensors must react identically and must be done particularly carefully. The surfaces of the Faraday'screen and of the sensor face to face as well as the distance between them must be exactly the same.

When one sensor is active, the other must not influence it and must be insulated. When the sensors are swapped the perturbation is the same, a solution [15] is to apply the following procedure illustrated in Fig.18.

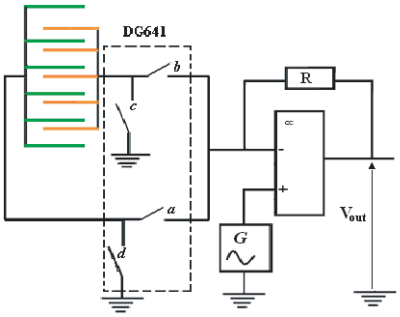


Fig. 18. Sensor working cycle.

1) Start: 4 toggle switches a, b, c and d are switch off.
2) c and d are switch on: both sensors are grounded and are electrically neutral.
3) c and d are switch off: both sensors are electrically insulated and they are not charged.
4) a is switch on: the sensor 1 is active.
5) a is switch off: the sensor 1 is no more active.
6) switch c is switch on: the sensor 1 is electrically neutral.
7) switch c is switch off: the sensor 1 is electrically insulated and it is not charged.
8) b is witch on: the sensor 2 is active.
9) b is switch off: the sensor 1 is no more active.
10) d is switch on: the sensor 1 is electrically neutral.
11) d is switch off: the sensor 1 is electrically insulated and it is not charged.
12) The cycle goes on to the step 4.

### C. Design of the sensor orientation

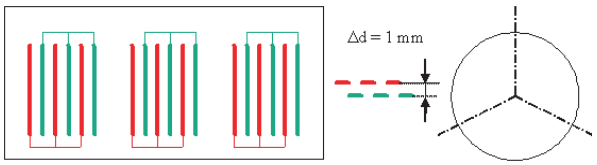


Fig. 19. Sensors disposition on a robot arm.

To increase the detection efficiency, 3 pairs of sensors arranged as a three branches star (angle of 120° between two branches) were spread out on each arm as shown in Fig.19. This architecture is usual for interdigital sensors [3], [14].

### D. Connection sensor - linear amplifier

The connection between the sensor and the linear integrated amplifier has to be done very carefully. Indeed, a simple

electric wire, connecting the sensor to the amplifier would behave like a sensor and would come to sully measurements. To circumvent this problem :

- the inverting input of the amplifier is directly welded onto the sensor, thus there is no wire of connection (the amplifier is off-set on the sensor).
- or a shielded cable is connected to the inverting input and its shielding to the non-inverting input as in Fig.20. Thus wire of connection and shielding [11] have the same potential since the sensor and the capacitive coupling due to the wire itself is not translated any more by the electronic circuit. In this case, the self capacitance of the shielded connection wire $C_{FLB}$ must be considered in the expression of $C_{iS}(d)_{exp}$ for the active sensor credit.

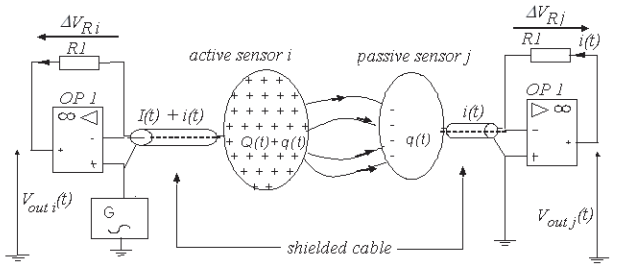


Fig. 20. Connection between the sensor and the linear integrated amplifier.

### *E. Stability of the sinusoidal oscillator*

The oscillator must be stable regarding its frequency and its amplitude, its parameters were fixed at $F$ = 10 kHz $\pm$ 0.1 Hz and $V_{in}$ = 2 V $\pm$ 0.0001 V.

## VII. Discussion and Conclusion

A novel low cost sensing set-up has been built and tested for estimating the distance between sensors and an intruder. An interdigital configuration has been fabricated and experiment results show it is able to discriminate intruders such as a human being or metallic objets. Also it is able to consider the capacitance variations that a machine induces on itself due to its variable geometry. That low cost system can be implemented to improve the safety in robotized production sites. Note that the dust is a recurring problem with such a system, a solution consists in observing the drifts of the coefficients $C_{is}$ in their initial positions. Then the system must be reboot for each cycle start.

## Acknowledgment

The authors thank F. Grimbert and P. Galland of the SAIC of the UNIVERSITY OF REIMS CHAMPAGNE ARDENNE for supporting us to deposit a patent INPI n°2898825.

## References

[1] B. Pottier, *"Etude et réalisation d'un Détecteur de Proximité capacitif dédié à la Sécurité des Personnes"*, PhD Thesis URCA France, 1992.
[2] B. Pottier, L. Rasolofondraibe, D. Nuzillard, INPI n°2898825, 2007.
[3] A.V. Mamishev, K. Sundara-Rajan, F. Yang, Y. Du and M. Zahn, "Interdigital Sensors and Transducers", *IEEE Proc.* vol.92, no.5, pp.808-845, may 2004.
[4] L. K. Baxter, *"Capacitive Sensors Design & Applications."* New York: IEEE Press, 1997.
[5] M. Gasulla, L. Xiujun, G. C. M. Meijer, H. Van Brussel, and R. Puers, "A contactless capacitive angular-posirion sensor," *IEEE Sensors Journal,* vol.3, no.5, pp.607-614,oct. 2003.
[6] A. Kimoto, S. Tsuji, and K. Shiada, "Noncontact Material Identification and Distance Measurement Using Effective Capacitance With CdS Cells," *IEEE Sensors Journal,* vol.7, no.10, pp.1440-1146, oct 2007.
[7] L. Bävall, N. Karlsson, "Capacitive Detection of Humans for Safety in Industry : a numerical and experimental Investigation", *Measurement Science & Technology,* 9(3), pp.505-509, 1998.
[8] B. Pottier, L.Rasolofondraibe, D.Nuzillard, "Capacitive Protection System for Robot dedicated to the Safety of Humans", *IECON06 IEEE*, Paris-France November 2006.
[9] N. Gershenfeld, J. Smith, "Method and Apparatus for characterizing Movement of a Mass within a defined Space", United States Patent n°6051981, april 2000.
[10] T. Kobayashi, "Proximity Sensor and Object detecting Device", United States Patent n°0080755 A1, may 2003.
[11] T. Zimmerman, J. Smith, J. Paradiso, D. Allport, N. Gershenfeld, "Appling Electric Field Sensing to Human-Computer Interfaces", in Proceedings of CHI'95; *ACM Conference on Human Factors in Computing Systems,* pp.280-287, IEEE SIG 1995.
[12] X. Li and G.C.M. Meijer, "Elimination of shunting Conductance Effects in a Low-Cost Capacitive-Sensor Interface",*IEEE Transactions on Instrumentation & Measurement,* vol.49, no.3, pp.531-534, 2000.
[13] OPA129 datasheet: http://www.datasheetcatalog.com/datasheet_ pdf/O/P /A /I/OPA129.shtml
[14] S.C. Mukhopadhyay and C. P. Gooneratne, "A Novel Planar-Type Biosensor for Noninvasive Meat Inspection", *IEEE Sensors Journal*, vol.7, no.9, pp.1340-1346, 2007.
[15] DG641 datasheet: http: //pdf.chinaicmart.com /DG6 /DG641.pdf

**Bernard Pottier** received his mechanical engineering diploma from INSA Lyon in 1983 and his PhD. degree in electronics from the University of Reims - Champagne Ardenne in 1989.
He is an assistant professor since 1991 at Reims - Champagne Ardenne University as member of the CReSTIC laboratory. His main topics are instrumentation, mechanical engineering and signal processing in relationship with blind source separation and independent component analysis.

**Lanto Rasolofondraibe** received his PhD. degree in electronics from the University of Reims - Champagne Ardenne in 1995.
He is an assistant professor since 1999 at Reims-Champagne-Ardenne University as member of the CReSTIC laboratory. His main topics are instrumentation, vibratory analysis and signal processing and in relationship with blind source separation and independent component analysis.

**Danielle Nuzillard** received her PhD. degree in electronics from the University of Paris XI, Orsay, in 1986.
She is a full professor since 2003 at Reims-Champagne-Ardenne University as member of the CReSTIC laboratory. Her main topics are instrumentation, signal and image processing in relationship with blind source separation and independent component analysis.